Proceedings of ICFDP9:
Ninth International Congress of Fluid Dynamics & Propulsion
December 18-21, 2008, Alexandria, Egypt

ICFDP9-EG-248

STUDY OF USING VORTEX BREAKDOWN IN VORTICAL FLOW FIELD AT THE OUTLET OF PROPELLANT TANKS

Hasan Karimi
Associate Professor of Aerospace Engineering
K.N.Toosi University of Technology

Mahdi N.Mahyari
M.Sc. Student of Mechanical Engineering
K.N.Toosi University of Technology

Hasan Naseh
M.Sc. Student of Aerospace Engineering
K.N.Toosi University of Technology

Mehran Mirshams
Assistant Professor of Aerospace Engineering
K.N.Toosi University of Technology

ABSTRACT

In this study, a 2-D, axis symmetric, transient and two-phase numerical model is created to evaluate the propellant critical height. Also, some experiments are conducted to determine the effect of use of vortex breakdowns at the outlet of liquid-rocket tanks on the critical height and residual mass of propellant. As the result of reducing the critical height and residual mass of propellant, orbital altitude of launch vehicles will be increased. The software titled *Launch Vehicle Conceptual Design* (LVCD) is applied to illustrate the improvement scales of ballistic parameters. It is found that vortex breakdowns can improve the launch vehicles in terms of both performance enhancement and cost reduction. Finally, simulation for existing Multi-Stage Launch Vehicle (MSLV) is examined to illustrate 15% increase achievement in launch vehicle orbital capabilities due to vortex breakdown application at the outlet of liquid-propellant tanks.

KEYWORDS:

vortex breakdown, critical height, propellant, launch vehicle.

INTRODUCTION

It is an indisputable fact that some of the important results in the space industry are due to the advances made in Launch Vehicle (LV) design and technology. Feasible algorithms for LV optimization and/or improvement are required. It is apparent that reduction of the costs while keeping the LV weight at a minimum is the prime goal of any space vehicle/equipment design.

Generally, vortex formation at the outlet of a tank is a significant and undesirable phenomenon. Vortex formation in flux fields with either free surface or near a sink (in several systems such as the water supply systems or tanks of launch systems of satellites) is of great importance. For example, as the tank draining nears the end, some free surface disturbances may occur as shown in Figure (1.a); this leads to sudden appearance of gases in the out flowing liquid as depicted in Figure (1.b).

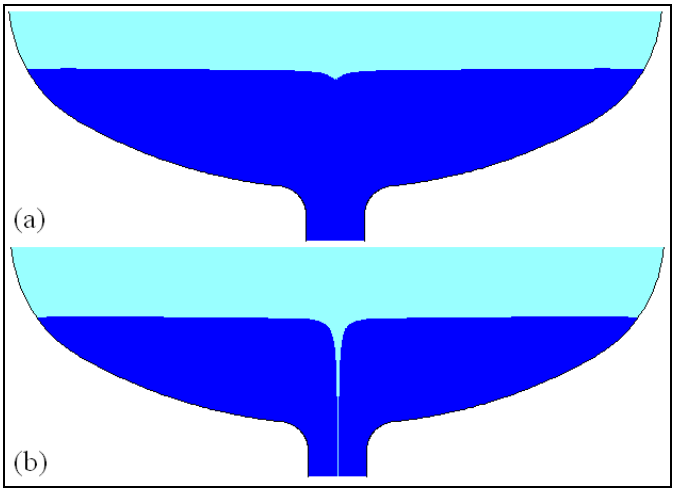

Figure 1. Gas inclusion into the intake: (a) dimple height (b) critical height.

Gas presence in the liquid causes a sudden increase in turbo-pump rotational velocity. Because feed pump operation is

not recommended in such conditions, the engine must be stopped before any gas ingestion occurs. A common solution to avoid this problem is to consider overcharging the propellant tanks followed by adequate discharging until the propellant height reaches its critical value. Residual mass of liquid will remain in the tank. The quantity of diphasic residual mass depends on the dynamic conditions during the draining process. In this way, flight weight will be increased, and efficiency is lowered. The purpose of this research is to reduce the excess flight weight (which includes dry structure and propellant weight) while improving the performance of Multi-Stage Launch Vehicles.

Some analytical and experimental studies have been conducted on vortical flows in hydraulic engineering. In these cases free surface is located too close to the outlet as is done in a power plant's intake [1, 2]. A simple device is suggested for preventing vortex formation in a small scale cylindrical container by Lakshmana Gowda et al. [3, 4]. Effect of initial tangential velocity and intake eccentricity on critical height of flow was examined by Piva et al. [5]. Also, an unsteady 3D numerical model is created to simulate the flow field in oxidizer tank near the vortex breakdown for ARIANE 5 launch vehicle (see Figure 2) [6]. But, no research has been published to evaluate the effect of vortex breakdowns on performance of a launch vehicle, until now.

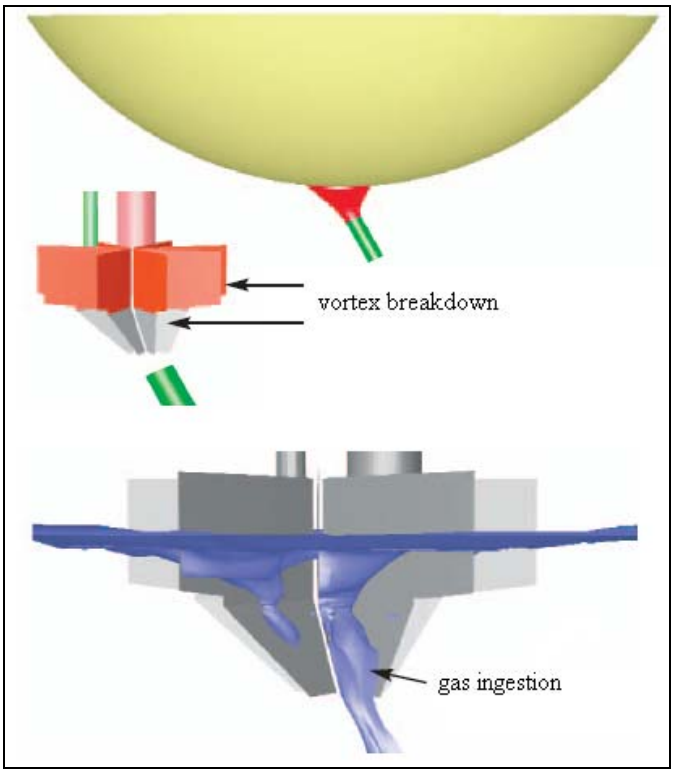

Figure 2. Geometry of ARIANE 5 oxidizer tank numerical modeling of vortical flow at the outlet [6].

"LVCD" code has been created to illustrate the effect of vortex breakdown on improvement of launch vehicle performance. This code is capable to compute optimized mass and energy parameters for multi-stage launch vehicles.

Mark J. Lewis et al. [7], performed design and build of a launch vehicle which could deliver a 100 kg payload to 200 km orbit. In that work, the design is based on statistical modeling, and no optimization of design parameters is carried out. Shyama Chakroborty et al. [8], Microcosm, and the Scorpius® Space Launch Company are developing a family of expendable launch vehicles that will lower the costs. On the other hand, it allows responsive access to space. In that work also no optimization in design parameters is carried out. A methodology based on fundamental beam structural analysis is developed for the rapid estimation of the load-bearing structural weight of the launch vehicle fuselage and integral propellant tanks by Virgil L. Hutchinson, Jr. et al. [9]. In that work, no effect of residual propellant mass on estimation of structural weight is considered.

In the Launch Vehicle Conceptual Design (LVCD) software, the results of various researches are employed to develop a conceptual design algorithm for a launch vehicle; a launch vehicle with optimized major design parameters would be the outcome of the developed algorithm.

DIMENSIONAL ANALYSIS

For the purposes of the present study, let the critical height be defined as the submergence of the outlet at which incipient air entrainment is possible. Treating the critical height as the dependent variable, the following functional relationship may be written.

$$h_{cr} = f_1\left(d, D, \mu, \rho, \sigma, \upsilon, g\right) \tag{1}$$

By choosing d, ρ and υ as the repeating variables and doing dimensional analysis of the variables of equation (1), the following is obtained.

$$\frac{h_{cr}}{d} = f_2\left(\frac{D}{d}, \frac{\rho \upsilon d}{\mu}, \frac{\upsilon}{\sqrt{gd}}, \frac{\rho \upsilon^2 d}{\sigma}\right) \tag{2}$$

Since the parameter D / d is great enough in the tests, the effect of the boundary of the tank on vortex formation is negligible and can be dropped from equation (2), i.e.

$$\frac{h_{cr}}{d} = f_3\left(Re, Fr, We\right) \tag{3}$$

It is necessary to find ranges for nondimensional parameters in equation (3) that h_{cr} / d is not a strong function of these parameters. This can be obtained analytically to reduce the number of the test iterations.

ANALYTICAL CONSIDERATION

The flow situation considered is depicted in Figure 1. For liquid motion in the vicinity of the vertical axis that is steady, axis-symmetric and laminar, the equations of motion for an incompressible fluid are

$$\frac{1}{r}\frac{\partial}{\partial r}(rv_r)+\frac{\partial v_z}{\partial z}=0 \tag{4}$$

$$v_r\frac{\partial v_r}{\partial r}+v_z\frac{\partial v_r}{\partial z}-\frac{v_\theta^2}{r}=-\frac{1}{\rho}\frac{\partial P}{\partial r}+\ldots +\nu\left(\frac{\partial^2 v_r}{\partial r^2}+\frac{1}{r}\frac{\partial v_r}{\partial r}-\frac{v_r}{r^2}+\frac{\partial^2 v_r}{\partial z^2}\right) \tag{5}$$

$$v_r\frac{\partial v_\theta}{\partial r}+v_z\frac{\partial v_\theta}{\partial z}+\frac{v_r v_\theta}{r}=\ldots =\nu\left(\frac{\partial^2 v_\theta}{\partial r^2}+\frac{1}{r}\frac{\partial v_\theta}{\partial r}-\frac{v_\theta}{r^2}+\frac{\partial^2 v_\theta}{\partial z^2}\right) \tag{6}$$

$$v_r\frac{\partial v_z}{\partial r}+v_z\frac{\partial v_z}{\partial z}=-\frac{1}{\rho}\frac{\partial P}{\partial z}+\ldots +\nu\left(\frac{\partial^2 v_z}{\partial r^2}+\frac{1}{r}\frac{\partial v_z}{\partial r}+\frac{\partial^2 v_z}{\partial z^2}\right)+g \tag{7}$$

The model is obtained by superimposing a radial flow on a vortex flow given by

$$v_\theta=\frac{\Gamma_\infty}{2\pi r}f(r) \tag{8}$$

where Γ_∞ is the circulation in radius where is far enough from axis. Substituting equation (8) into equation (6) yields

$$v_r\frac{f'}{r}+\nu\frac{d}{dr}\left(\frac{f'}{r}\right)=0 \tag{9}$$

where $f'=df/dr$. Near the pipe entrance, the redial velocity component is nearly linear

$$v_r\cong -a\,r \quad r<r_\circ,\ z\le h_{cr} \tag{10}$$

By continuing from equation (4), the axial velocity near the pipe entrance is then given by

$$v_z=2a\,z \quad r<r_\circ,\ z\le h_{cr} \tag{11}$$

Note that v_r is given by equation (10), $f\to 1$ for $r\to\infty$, and v_θ has no singularity at $r=0$. Then by obtaining the solution of equation (9) and by substituting it into equation (8), a tangential velocity distribution is obtained as follows.

$$v_\theta=\frac{\Gamma_\infty}{2\pi r}f(r)=\frac{\Gamma_\infty}{2\pi r}\left[1-exp\left(-\frac{1}{2}\frac{a}{\nu}r^2\right)\right] \tag{12}$$

The maximum tangential velocity occurs at the distance r_c; this distance is measured from the axis, and it is given by

$$r_c^2=2.5\frac{\nu}{a} \tag{13}$$

Therefore, the maximum value of tangential velocity ($v_{\theta,c}$) is given by

$$v_{\theta,c}^2=0.00516\,\Gamma_\infty^2\frac{a}{\nu} \tag{14}$$

Equation (12) can be normalized by equations (13) and (14).

$$\frac{v_\theta}{v_{\theta,c}}=1.4\frac{r_c}{r}\left[1-exp\left(-1.25\left(\frac{r}{r_c}\right)^2\right)\right] \tag{15}$$

Figure (3) shows the variation of tangential velocity versus radial distance from equation (15).

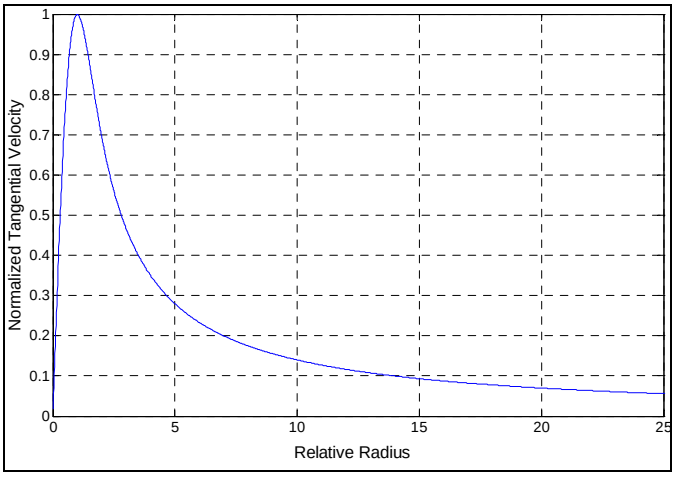

Figure 3. Normalized tangential velocity from equation (15) versus nondimensional radius.

The critical height is obtained from the pressure distribution and by substituting equations (10) and (11) into equations (5) and (7); then integrate the resulting equation.

$$P=P_\circ+\int_0^r\rho\frac{v_\theta^2}{r}dr-\frac{1}{2}\rho a^2r^2 \tag{16}$$

where $P_\circ$, the pressure at the tip of vortex due to surface tension, is Equal to $-2\sigma/r_c$. For distances beyond r_c, P tends to hydraulic pressure. The third term on the right hand side of equation (16) is small compared with the second term for $r<r_\circ$. Integrating from axis to $r=r_\circ$ and by using equations (15) and (16), the following equation is obtained.

$$h_{cr}=-\frac{2\sigma}{r_c\rho g}+3.4\left[1-0.5\left(\frac{r_c}{r_\circ}\right)^2\right]\frac{v_{\theta,c}^2}{2g} \tag{17}$$

where r_c is given by equation (13) and from equation (11): $a=\upsilon/2h_{cr}$. The radius ratio in equation (14) is $5\nu h_{cr}/\left(\upsilon r_\circ^2\right)$; this is a number so small that the value of bracket in equation (17) can be taken to be unity. By using equations (13) and (14) with $a=\upsilon/2h_{cr}$, equation (17) reduces to the following equation.

$$h_{cr}^2=-0.9\frac{\sigma}{\rho g}\sqrt{\frac{\upsilon h_{cr}}{\nu}}+0.0043\frac{\Gamma_\infty^2\upsilon}{g\nu} \tag{18}$$

In terms of nondimensionalized parameters, this equation would be of the following form.

$$\left(\frac{h_{cr}}{d}\right)^2 = -0.89\,Fr^2\,Re^{1/2}\left(\frac{h_{cr}}{d}\right)^{1/2} We^{-1} + \ldots + 0.0026\,Fr^2\,Re\,N_\Gamma^2 \quad (19)$$

A criterion for neglecting effects of surface tension may be established by requiring that ratio between the surface tension and circulation terms in equation (17) be less than 10%. Thus

$$\frac{\rho v_{\theta,c}^2 r_c}{\sigma} > 12 \quad (20)$$

Substituting equations (13) and (14) into equation (20) leads to the following equation.

$$We > 720\,Fr^{1/2}\,N_\Gamma^{-3/2}\,Re^{-1/4} \quad (21)$$

The values of $Fr^{1/2}$, $N_\Gamma^{3/2}$ and $Re^{1/4}$ are of the order of 1, 0.1 and 10, respectively, under the typical model conditions; therefore, the criterion to neglect the surface tension will be $We > 720$.

Also, a criterion for neglecting effects of viscosity can be established by requiring that turbulent viscosity be greater than 5ν. This condition provides less than 10% effect on critical height. It follows from equation (18) that without the surface tension term, this criterion is met when the following condition is satisfied.

$$Re > 1.1\times10^3\left(\frac{h_{cr}}{d}\right)^2 \frac{gd^3}{\Gamma_\infty^2} \quad (22)$$

The value of $(h_{cr}/d)(\sqrt{gd^3}/\Gamma_\infty)$ is of the order of 10, and criterion to neglect viscous effects is $Re > 1.1\times10^5$.

Under the conditions where $Re > 1.1\times10^5$ and $We > 720$, equation (19) can be simplified as follows.

$$\frac{h_{cr}}{d} = 1.55\,Fr^{1/3} \quad (23)$$

Note that there is no imposed circulation on the flow field inside the tank, and critical height is free from the circulation number in this case.

NUMERICAL MODEL

Generally, vortex formation at the propellant tank outlet is a 3-D, unsteady, turbulent and two-phase phenomenon. So, a complete numerical solution will be time-consuming and expensive. Therefore, a 2-D, axis-symmetric, transient and two-phase numerical model created to simulate the flow field. Both Reynolds number and Weber number are greater than criteria mentioned before. According to equation (23), Froude number is the most effective parameter which affects on the critical height. Thus the numerical model should be run for various Froude numbers to show the variation of critical height.

Domain of the solution, generated structured mesh and boundary conditions are shown in Figure (4). Air enters to the inlet boundary with constant pressure and water will be expulsed with constant mass flow rate at the outlet. Solution continues while the volume fraction of water is equal to 1. Passing the air bubble through the outlet reduces the water volume fraction; therefore, the boundary condition at the outlet will not be satisfied and solution will be stopped.

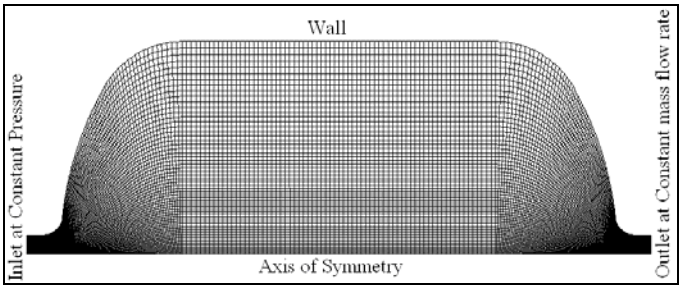

Figure 4. Structured mesh with 30040 elements.

The tracking of the interface between the phases is accomplished by the solution of a continuity equation for the volume fraction of the phases. For the *i*th phase, this equation has the following form

$$\frac{\partial \alpha_i}{\partial t} + \vec{V}.\nabla\alpha_i = 0 \quad , \quad \sum_{i=1}^{2}\alpha_i = 1 \quad (24)$$

A single momentum equation is solved throughout the domain, and the resulting velocity field is shared among the phases. The momentum equation, shown below, depends on the volume fractions of all phases through the properties ρ and μ.

$$\frac{\partial\left(\rho\vec{V}\right)}{\partial t} + \nabla.\left(\rho\vec{V}\vec{V}\right) = -\nabla P + \ldots + \nabla.\left[\mu\left(\nabla\vec{V} + \nabla\vec{V}^T\right)\right] + \rho\vec{g} + \vec{F} \quad (25)$$

In general, for an n-phase system, the volume-fraction-averaged φ (like density or viscosity) takes on the following form

$$\varphi = \sum_{i=1}^{n}\alpha_i\varphi_i \quad (26)$$

By using a 2-D axis-symmetric model, critical height of the fluid can be estimated as a function of Froude number. But, investigation of the effect of the vortex breakdowns needs a fully 3-D numerical model. However, it is possible to show the effect of a circular plate located top of the intake on the flow field using a 2-D axis-symmetric model. Figure (5) shows a part of the unstructured mesh generated for this object.

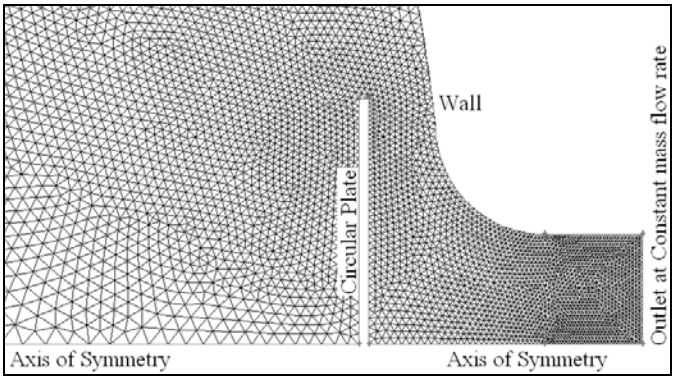

Figure 5. Unstructured mesh with 23095 elements.

$k-\varepsilon$ model is employed to simulate the turbulence in CFD code. A segregated solver used to solve the flow field equations, and SIMPLE algorithm applied to couple the pressure and velocity fields. Also, first order scheme used to discrete the convection terms of governing equations.
Figure (6) shows counter of velocity magnitude for both gas and liquid phases. Counter of tangential velocity illustrated in Figure (7). It is found that tangential velocity of a particle increases while it is moving towards the outlet. Figure (8) shows the formation of gas funnel at interface of phases. Figures (9, 10 and 11) are similar to three past figures, respectively but for the case that a circular plate (see Figure 5) located on top of the intake.

To show the effect of Reynolds number on numerical model Results, the variation of critical height was compared for $Re = 4.5\times10^5$ and $Re = 9.0\times10^5$ at $Fr = 3.882$. Results represented in Table (1) show that the effect of Reynolds number can be negligible.

Table 1. Effect of Reynolds Number on critical height at Fr = 3.882

	Reynolds Number		Error
	$Re = 4.5\times10^5$	$Re = 9.0\times10^5$	
Without plate	1.83	1.95	5.6%
With plate	1.04	1.07	2.8%

Also, mesh independency of the numerical solution was examined by comparing the results of a coarse mesh with a finer mesh. The errors in Table (2) show that the mesh used in the model is fine enough.

Table 2. Effect of mesh size on critical height at Fr = 3.882

	Number of elements in mesh		Error
	20×10^3	30×10^3	
Without plate	1.84	1.83	0.72%
With plate	1.07	1.04	2.6%

EXPERIMENTS

Experiments are conducted to measure critical height in propellant tanks with and without vortex breakdown. Fortunately, the values of Reynolds and Weber numbers for both model and prototype conditions are greater than the mentioned criterion (see Table 3). Thus, experiments are dedicated to investigate the effect of Froude number on critical height for various outlets. Froude number is a parameter which can describe the flight conditions in stand model. Under the flight conditions, Froude number must be define as a function of axial acceleration (a_x), pitch angle (θ) and local gravity (g) as is described below.

$$Fr = \frac{\upsilon}{\sqrt{(a_x + g\sin\theta)d}} \tag{23}$$

Equation (23) can be simplified to $\upsilon/\sqrt{gd}$ when both a_x and θ are equal to zero.

The tests are carried out using a transparent cylindrical tank with an internal diameter of 1.25 m and a height of 2.0 m with a centrally located internal diameter of 112 mm (see Figure 13). The working liquid in the experiments is water at room temperature. Effects of four devices are investigated as vortex breakdown in the experiments

1. A circular flat plate with diameter of $3d$.
2. A circular flat plate with diameter of $3d$ with four radial blades (see Figure 14.a).
3. A circular flat plate with diameter of $3d$ with eight radial blades.
4. A circular flat plate with porous wall (see Figure 14.b).

Table 3. Characteristic parameters for a two-stage launch vehicle.

Parameter	unit	1st stage		2nd stage	
		Fu	Ox	Fu	Ox
ρ	kg/m^3	805	1603	795	1458
$\mu\times10^4$	$kg/m.s$	8.24	19	5.6	4.2
$\sigma\times10^3$	N/m	54	_	24.1	25.1
$\dot{m}$	kg/s	31.1	109	5.3	7.6
υ	m/s	3.92	6.93	6.16	4.86
a_x	m/s^2	55		65	
θ	deg	25		0	
Fr	_	1.52	2.69	3.97	3.13
$Re\times10^{-5}$	_	4.3	6.6	3.2	6.2
$We\times10^{-4}$	_	5.2	_	4.6	5.1

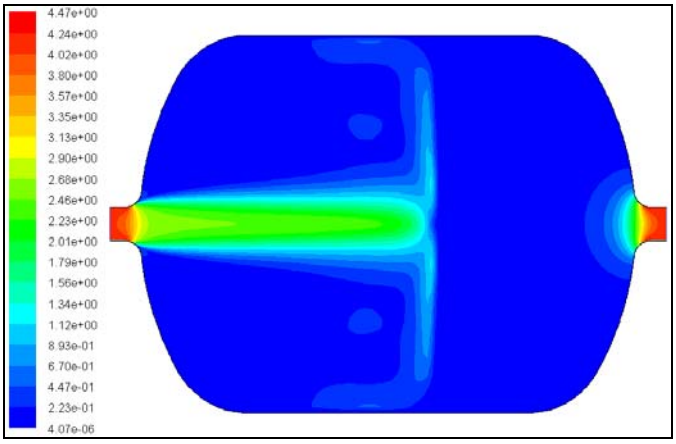

Figure 6. Counter of velocity magnitude (m/s).

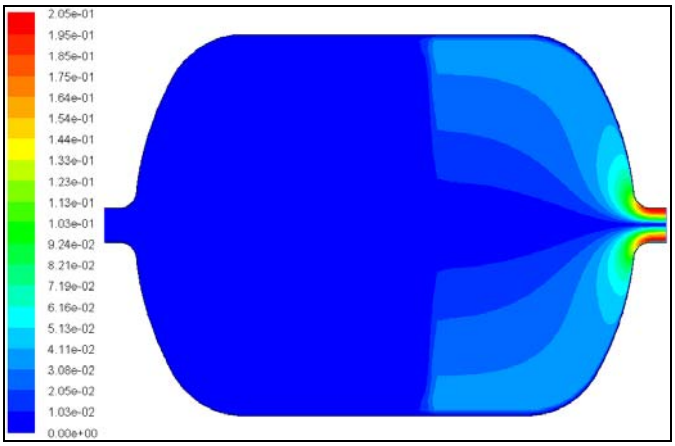

Figure 7. Counter of tangential velocity (m/s).

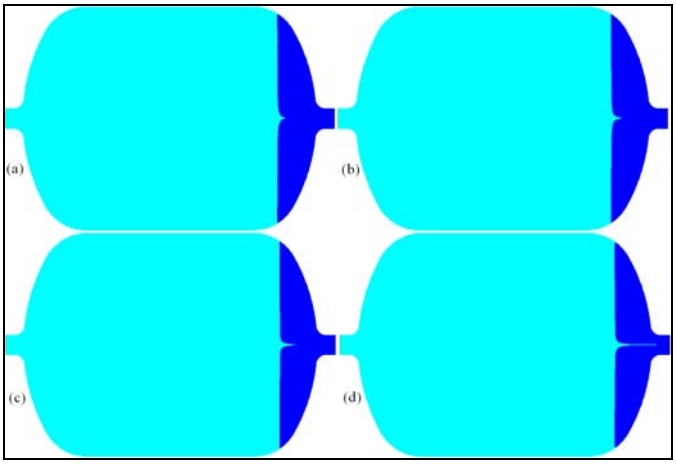

Figure 8. Counters of Phase: variation of interface during the time and gas penetration to outlet.

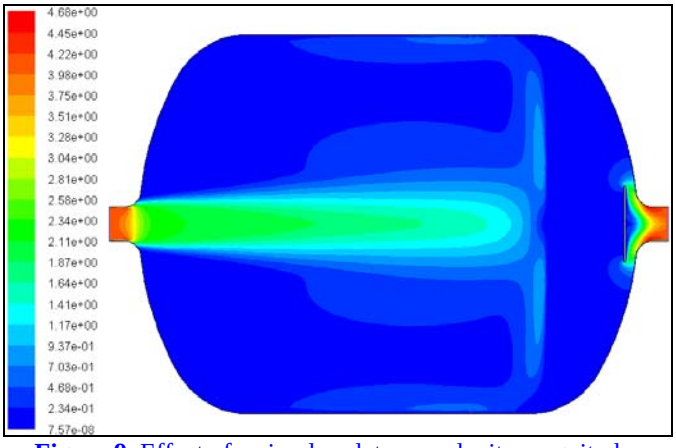

Figure 9. Effect of a circular plate on velocity magnitude**.**

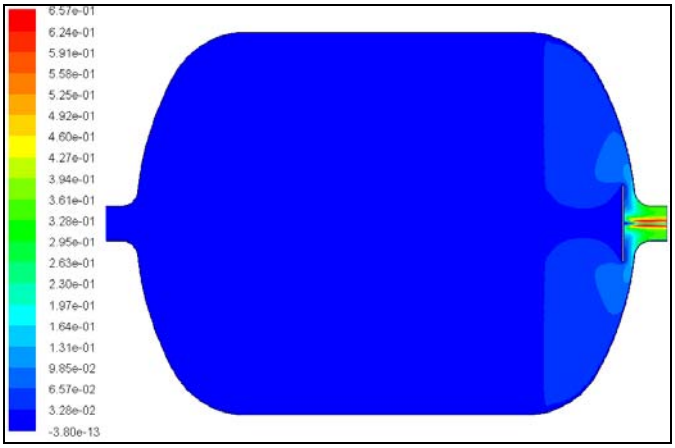

Figure 10. Effect of a circular plate on tangential velocity.

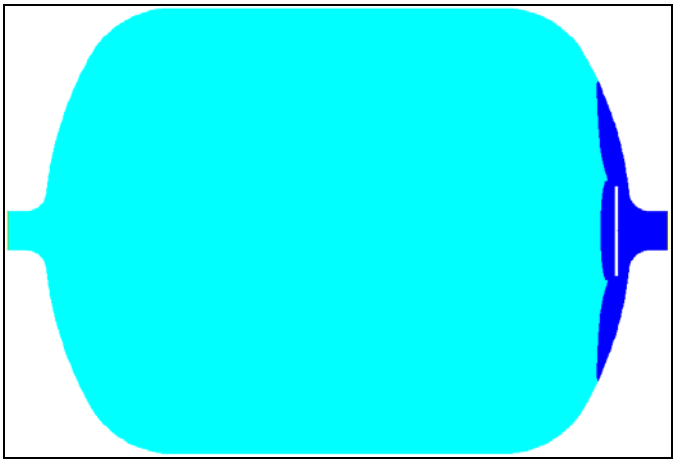

Figure 11. Effect of a circular plate on interface disturbance and reduction in critical height.

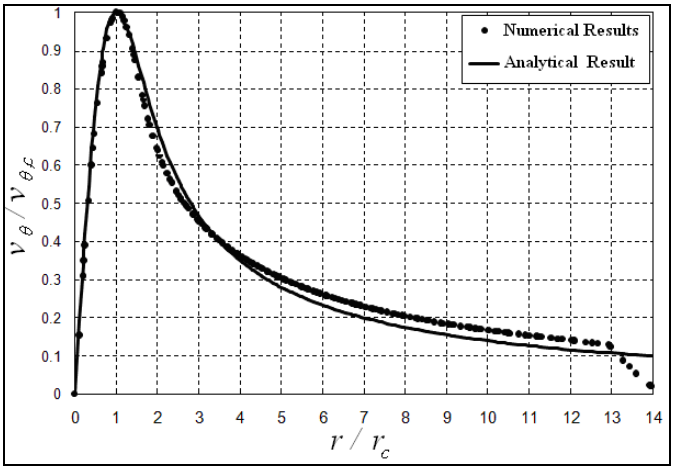

Figure 12. Comparison of analytical and numerical solutions for tangential velocity distribution.

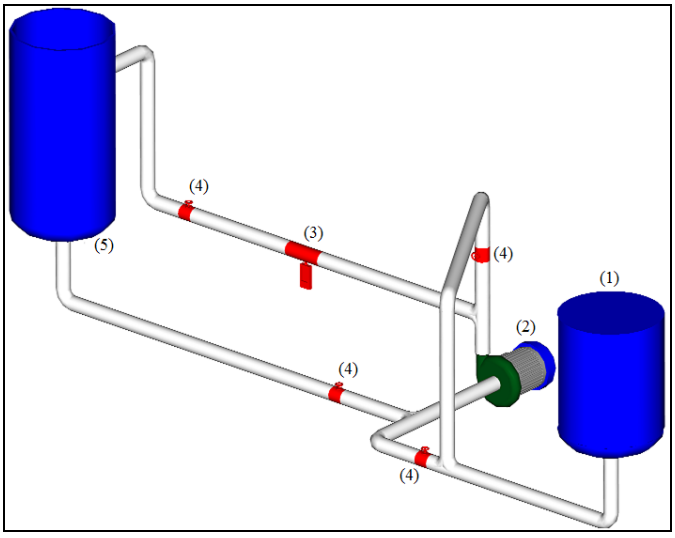

Figure 13. Experimental setup layout: (1) propellant tank, (2) pump, (3) magnetic flow meter, (4) butterfly valves, (5) reservoir tank.

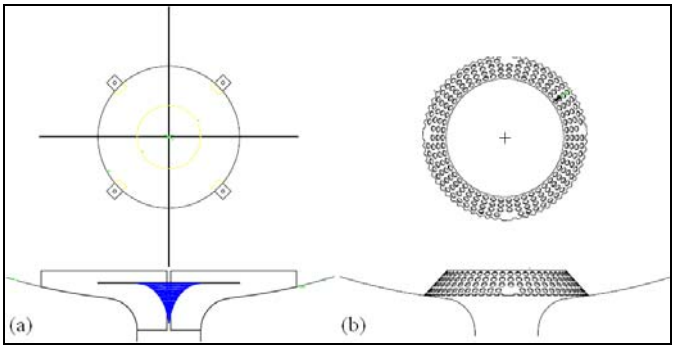

Figure 14. Two types of vortex breakdown.

Variations of nondimensionalized critical height versus Froude number for the above four cases are illustrated in Figure (15).

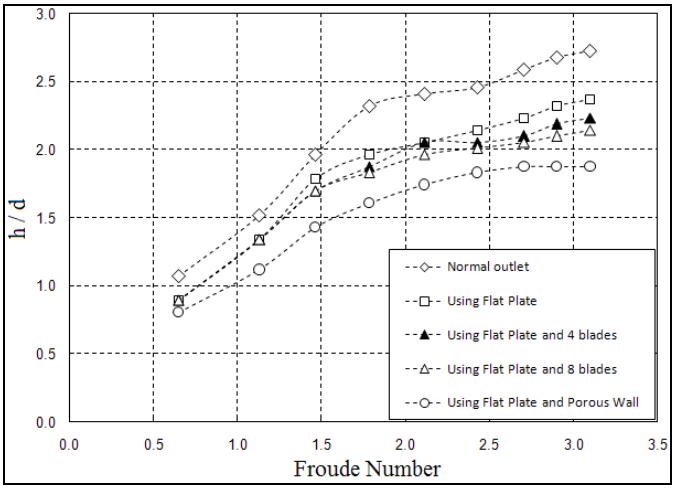

Figure 15. Nondimensional critical height versus Froude number and effect of vortex breakdowns.

LVCD SOFTWARE DEFINITION

Launch Vehicle Conceptual Design (LVCD) software based on multi-parameter optimization idea has been programmed. The main objectives of this software are reduction of the cost and time of conceptual design phase. This software is user friendly such that an operator familiar with fundamental of design and launch vehicle mass–energy equations and with primary training operator will be capable to work with LVCD. The algorithm used in LVCD, is based on combinational optimization of major design parameters. To this end, ten sub-algorithms have been used in this design approach (see Figure 16). In this software, structure, propellant and mass distribution calculations of different stages to launch maximum payload mass to the orbit, pitch program trajectory to achieve the maximum final velocity, providing minimum velocity loss due to gravity, and minimum axial acceleration of various stages of launch vehicle will be optimized as the results of the presented approach. The optimization process is performed subject to the restrictions. Also, the performance index is optimized in a mutual iteration mechanism (multi-parameter optimization). Evaluation and verification of the presented method is performed using available data of two and three-stage launch vehicles.

The LVCD includes five conceptual design modules as the following

1. LV mass determination
2. Propulsion system selection
3. Flight trajectory simulation
4. LV sizing
5. LV sub-system specifications

LV will be optimized based on the interaction between above mentioned modules to determine the design parameters. The optimization process is performed subject to the restrictions and available technologies. In LVCD software, design calculation initiated based on mass and energy coefficients or technology factors that obtained from statistical database. Along LVCD algorithm iterations, technology factors will be optimized. Figure (16) shows the detailed flow chart used in LVCD software.

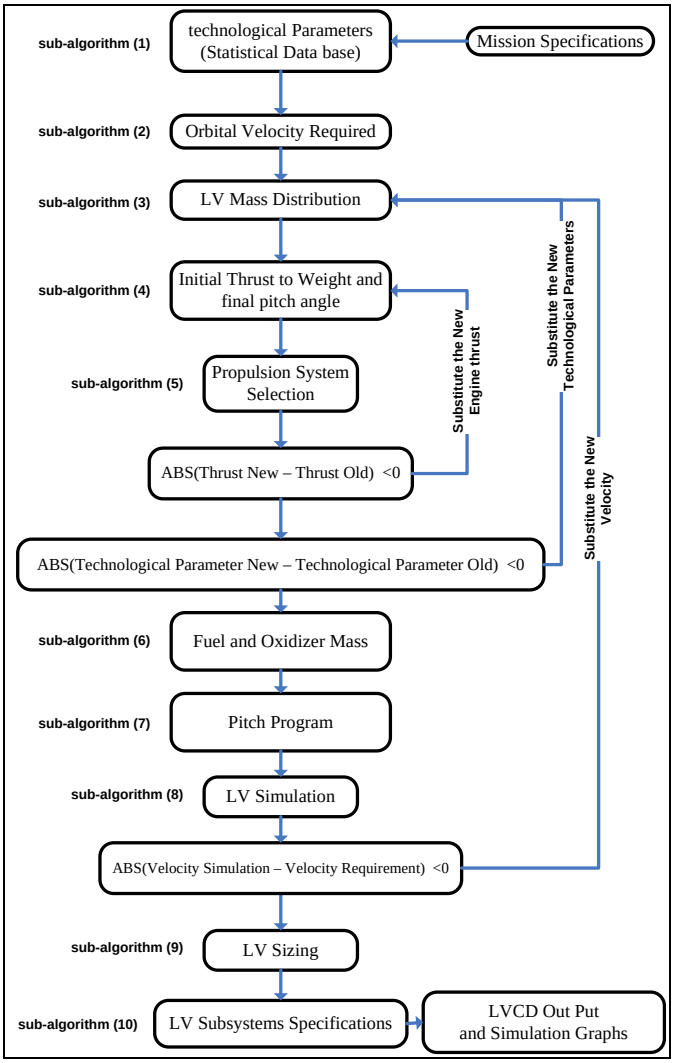

Figure 16. LVCD Flowchart.

Numerous factors of technology affect the LV ballistic capabilities. The most important of these factors follow

1. Tank to propellant mass ratio for various stages of LV
2. Residual propellant to total propellant mass ratio for various stages of LV
3. Final stage to initial stage mass ratio for various stages of LV
4. Thrust to weight ratio for various stages of LV

With use of vortex breakdown at the outlet of liquid-propellant tanks for a typical propulsion system, factors (1) to (3) will be reduced and factor (4) will be enhanced.

IMPROVEMENT SCALES ON LAUNCH VEHICLE PARAMETERS

The ultimate goals of this effort are to improve the performance of a MSLV and to simulate the LV. Results of simulation show that use of vortex breakdown at the outlet of liquid-propellant tanks leads to reduction in both dry structure and propellant weight and enhancement in engine burning time, thrust to weight ratio, axial acceleration (especially in upper stages), velocity and orbital altitude. LVCD is used to illustrate these improvements for a two-stage launch vehicle.

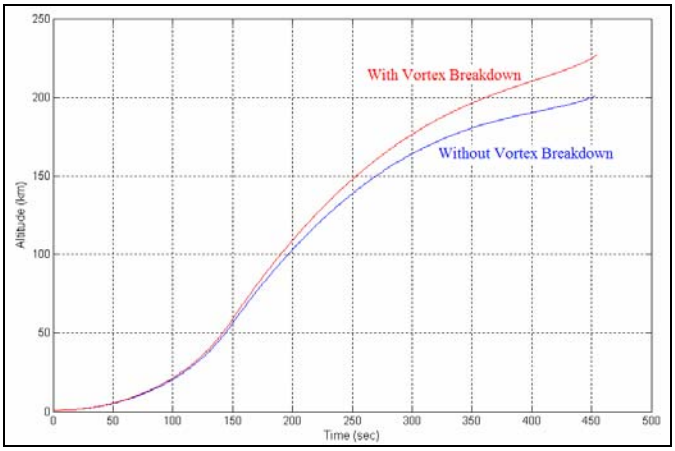

Figure 17. Improvement in orbital altitude.

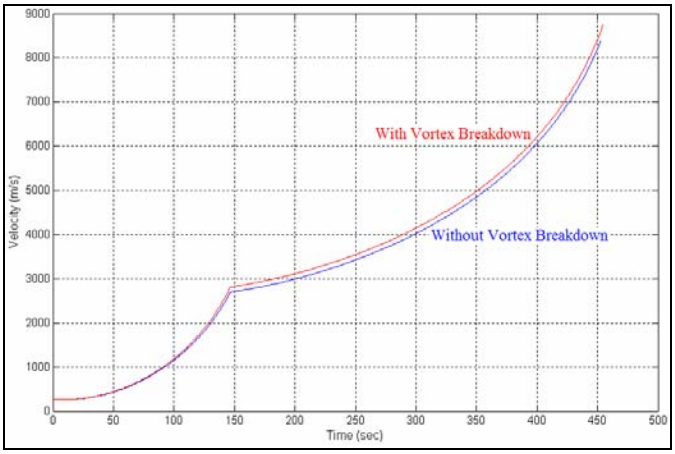

Figure 18. Improvement in velocity.

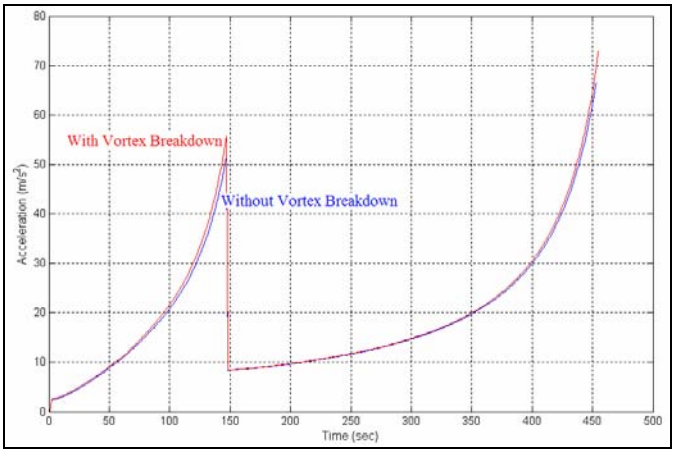

Figure 19. Improvement in axial acceleration.

CONCLUSION

Analytical investigation of this work indicates that viscous and surface effects of free-surface vortices may be neglected when the intake Reynolds number and Weber number are greater than 1.1×10^5 and 720, respectively. In the experiments, critical height of fluid is considered as a function of Froude number and outlet type. Results show a 13% decrease in critical height via installation of a flat plate with diameter of $3d$ at the vicinity of intake. Also, by adding four blades to flat plate (as shown in Figure 14.a), a 20% decrease in critical height is noticed. It is possible to achieve a 30% decrease by using a flat plate with porous wall (as shown in Figure 14.b). In the last case, the mass of mentioned two-stage LV may be reduced by 280 kg and results of LVCD simulation show a 15% increase in orbital altitude (see Figure 19).

NOMENCLATURE

The following symbols are used in this paper:

a	factor of proportionality in equation (10)
a_x	axial acceleration of LV at the end of each stage
d	inner diameter of intake pipe
D	diameter of tank
f	function
$\vec{F}$	body force vector
Fr	Froude number
g	gravitational acceleration
h_{cr}	critical height
$\dot{m}$	mass flow rate
N_Γ	circulation number
P	pressure
$P_\circ$	pressure at the tip of vortex
r,θ,z	radial, tangential and axial coordinates
r_c	radial distance of maximum tangential velocity
$r_\circ$	intake pipe radius
Re	Reynolds number
t	time
υ	mean velocity at the tank outlet
v_r, v_θ, v_z	radial, tangential and axial component of velocity
$v_{\theta,c}$	maximum tangential velocity
$\vec{V}$	velocity vector
We	Weber number
α_i	volume fraction of ith phase in each cell
φ	volume-fraction averaged of physical properties of phases in equation (26)
φ_i	volume fraction of ith phase
Γ_∞	circulation at the far field
ν	kinematic viscosity
θ	pitch angle of LV at the end of each stage
ρ	density
σ	surface tension of liquid

ACKNOWLEDGMENTS

The authors are grateful to Dr. H. Parhizkar, M. Mohseni, A. Kalabkhani, A.Hadi Sadeq and Dr. A. Nasir Harand for their helpful comments and support.

REFERENCES

Some of references used in this paper are as the following:

[1] J. E. Hite and W. C. Walter, "Velocity of Air Core Vortices at Hydraulic Intakes", *Journal of Hydraulic Engineering*, Vol.120, No.3, pp.284-297, 1994.

[2] M. Maleewong, J. Asavanant and R. Grimshaw, "Free Surface Flow Under Gravity and Surface Tension Due to an Applied Pressure Distribution: I Bond Number Greater Than One-Third", *Journal of Computational Fluid Dynamic*, Vol.19, No.4, pp.237-252, 2005.

[3] B. H. Lakshamana Gowda, "Draining of Liquid from Tanks of Square or Rectangular Cross Sections", *Journal of Spacecraft*, Vol.33, No.2, pp.311-312, 1995.

[4] S.Mizuki, B. H. Lakshamana Gowda and T. Uchibaba, "Visualization Studies using PIV in a Cylindrical Tank with and without Vortex Suppressor", *Journal of Visualization*, Vol.6, No.4, pp.337-342, 2003.

[5] M. Piva, M. Iglesias, P. Bissio and A. Calvo, "Experiments on Vortex Funnel Formation During Drainage", *Physica A*, 329, pp.1-6, 2003.

[6] "Focus on CFD for the Ariane 5 Launcher", Fluent News, 2005.

[7] Mark J. Lewis, Tharen Rice, "Design of University Launch Vehicle System", *Journal of AIAA*, Department of Aerospace Engineering, University of Maryland at College Park, 1992.

[8] Shyama Chakroborty, James R. Wertz, Robert Conger, "The Scorpius Expendable Launch Vehicle Family and Status of the Sprite Small Launch Vehicle", *The 1st Responsive Space Conference*, April 1-3, 2003.

[9] Virgil L. Hutchinson, Jr. and John R. Olds , "Estimation of Launch Vehicle Propellant Tank Structural Weight Using Simplified Beam Approximation", *The 40th AIAA/ASME/SAE/ASEE Joint, Propulsion Conference and Exhibit,* Fort Lauderdale, Florida, July 11-14, AIAA 2004-366.

[10] N. Yildirim and F. Kocabas, "Prediction of Critical Submergence for an Intake Pipe", *Journal of Hydraulic Research*, Vol.40, No.4, pp.507-517, 2002.

[11] G. Echavez and E. McCann, "An Experimental Study on the Surface Vertical Vortex", *Experiments in Fluids*, Vol.33, No.3, pp.414-421, 2002.

[12] B. H. Lakshamana Gowda, P. J. Joshy and S. Swarnamani, "Device to Suppress Vortexing During Draining from Cylindrical Tanks", *Journal of Spacecraft*, Vol.33, No.4, pp.598-600, 1995.

[13] G. Haller, "on Objective Definition of a Vortex", *Journal of Fluid Mechanic*, Vol.525, pp.1-26, 2005.

[14] Thomas Alrutz and Markus Rutte, "Investigation of Vortex Breakdown over a Pitching Delta Wing Applying the DLR TAU-Code with Full, Automatic Grid Adaptation", *35th AIAA Fluid Dynamics Conference and Exhibit*, Toronto, Ontario Canada, AIAA 2005-5162.